J. Fluid Mech. (2003), *vol.* 491, *pp.* 285–300.
DOI: 10.1017/S0022112003005330 Printed in the United Kingdom

The effect of wall interactions in capillary-zone electrophoresis

By SANDIP GHOSAL

Department of Mechanical Engineering, Northwestern University,
2145 Sheridan Road, Evanston, IL 60208, USA

(Received 11 September 2002 and in revised form 23 April 2003)

Capillary-zone electrophoresis (CZE) is an efficient separation method in analytical chemistry. It exploits the difference in electrophoretic migration speeds between charged molecular species in aqueous solution when an external electric field is applied to achieve separation. In most cases the electrophoretic migration of species is also accompanied by a bulk electro-osmotic flow in the capillary due to the presence of a zeta-potential at the capillary wall. Adsorption of charged species at the wall could modify this zeta-potential in a non-uniform manner. This induces axial pressure gradients, so that the flow is no longer uniform over the capillary cross-section. The resulting shear-induced dispersion of the sample is a serious cause of band broadening in CZE particularly for species such as proteins and peptides which adsorb strongly on capillary walls. The problem of the spatio-temporal evolution of the sample concentration is studied in the presence of such wall interactions. An asymptotic theory is developed that is valid provided axial variations have characteristic length scales that are much larger than the capillary radius and temporal variations have a characteristic time scale much larger than the characteristic diffusion time over a capillary radius. These conditions are normally satisfied in CZE, except when the sample is close to the inlet, on account of the capillary length being very much larger than its radius. It is shown that the cross-sectionally averaged sample concentration obeys a one-dimensional partial differential equation. Further, the full three-dimensional concentration field may be calculated once the cross-sectionally averaged concentration field is known. The reduced system is integrated numerically and is shown to lead to predictions consistent with known observations on CZE in the presence of wall interactions.

1. Introduction

Capillary zone electrophoresis (CZE) is one of the methods employed in analytical chemistry for the separation of mixtures of chemical species by exploiting their different electrophoretic mobilities in aqueous solution (see Weinberger 2000; Jorgenson 1987 for a basic introduction). Since its discovery in the early 1970s, CZE has gained in popularity over more classical gel electrophoresis methods due to its superior resolution, short analysis times and small sample size requirement. In recent years, it has been the object of renewed interest due to the possibility of miniaturizing the device and integrating it in the 'Lab on a chip'. Such a device could in principle accomplish biochemical experiments at speeds that are orders of magnitude faster than are possible with existing technology while requiring extremely small quantities of samples and reagents (see e.g. Jakeway, de Mello & Russell 2000).

In its simplest form, a benchtop CZE device consists of a micro-capillary (characteristic diameter $10-100\,\mu m$ and $10-100\,cm$ long) connecting two reservoirs. The micro-capillary and both the reservoirs are filled with an ionic aqueous solution (the buffer) of known pH. (We only discuss 'free solution' CZE as opposed to separation modes where the capillary is filled with a sieving gel.) An electric potential difference ($\sim 30\,kV$) is applied between the inlet and outlet reservoirs by means of electrodes. The sample (analyte) is introduced as a plug near the inlet, and allowed to migrate towards the outlet due to the electro-osmotic flow induced by the electric field. Any particular species of molecule migrates with a velocity $u_e + v_e$ where u_e is the electro-osmotic velocity of the fluid in the capillary and v_e is the electrophoretic migration velocity specific to the chemical species. The electro-osmotic velocity may be calculated from the well known (Probstein 1994) formula:

$$u_e = -\frac{\epsilon_d \zeta_* E}{4\pi\mu} \tag{1.1}$$

(in CGS units) where ϵ_d is the dielectric constant of the liquid, ζ_* is the wall zeta-potential, E is the applied electric field and μ is the dynamic viscosity of the liquid. This formula is valid provided the zeta-potential is constant over the capillary wall and the Debye layer thickness is very much smaller than the capillary radius. The latter condition is usually satisfied in the applications we are concerned with. Since v_e is different for different species of molecules, the analyte separates into zones of homogeneous composition each with a characteristic electrophoretic mobility. A ultra-violet absorbance detector near the outlet end detects the arrival of each zone by monitoring the attenuation of ultra-violet light, which alters the electrical signal from a photodetector. The spectrum consist of a series of peaks in the electrical output. Each peak corresponds to the arrival at the detector of a zone which determines the electrophoretic mobility of the respective species.

Under ideal circumstances, the electro-osmotic flow profile is uniform (except in a very thin, ~ 1–$10\,nm$, boundary layer – the Debye layer – in which the flow speed decreases rapidly in order to satisfy the 'no-slip' boundary condition at the wall) over the capillary cross-section. Thus, there is negligible shear-induced dispersion so that 'diffusion limited' separation, where resolution is limited only by molecular diffusion, is potentially realizable. In practice, there are multiple known mechanisms of band broadening that prevent the diffusion-limited theoretical resolution from being realized (see the recent review by Gaš & Kendler 2000). In this paper we address the problem of dispersion caused by variability in the wall zeta-potential due to adsorption of analytes from the fluid stream. Perturbations due to such inhomogeneity not only alter the flow profile, but also the bulk flow rate, as shown by Anderson & Idol (1985) and Ghosal (2002*c*). Thus, in addition to band broadening, the elution times are altered making it difficult to calculate mobilities with accuracy. Adsorption also causes loss of some of the sample.

Analytical results on dispersion in the presence of wall adsorption have been presented by Gaš *et al.* (1995) and Štědrý, Gaš & Kendler (1995). Though their analyses take account of the fact that analyte is lost to the wall, the consequent modification of the zeta-potential and therefore the hydrodynamic flow field have been neglected. Indeed, the hydrodynamics is restricted to the trivial case of uniform flow at constant velocity independent of the adsorption process. However, recent theoretical as well as experimental work indicates that the modification of the the zeta-potential by adsorption, and the consequent perturbation of the hydrodynamic field, is an important, if not the principal cause of dispersion (Ghosal 2002*a*, *b*, *c*;

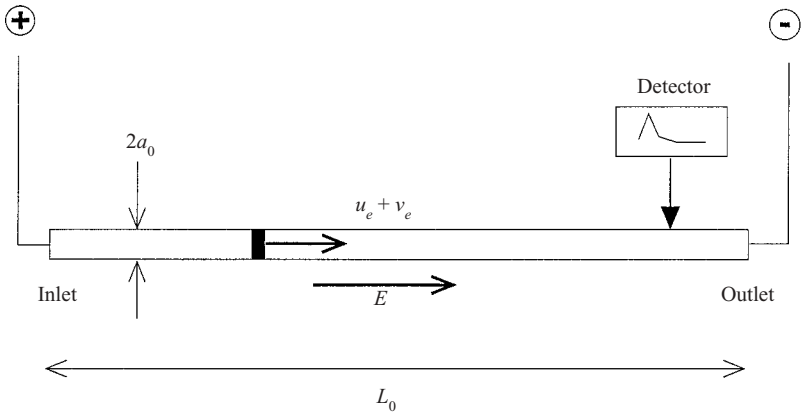

FIGURE 1. Schematic diagram illustrating the elements of a CZE apparatus.

Towns & Regnier 1992; Herr *et al.* 2000). Analyses of similar 'purely kinematic' models that neglect the perturbation in the hydrodynamic field have also been presented by Ermakov *et al.* (1995), Schure & Lenhoff (1993) and Zhukov, Ermakov & Righetti (1997). The most comprehensive study to date on the problem of wall adsorption and its consequences is an experimental one, due to Towns & Regnier (1992). These experiments together with their interpretation using simple fluid mechanical models have been discussed elsewhere by Ghosal (2002*a*, *b*).

The more restricted problem of determining the fluid flow in the presence of spatially varying zeta-potentials has been investigated in a number of recent studies. The first appears to be due to Anderson & Idol (1985), who derived an exact solution to the problem of electro-osmotic flow in the limit of zero Reynolds number and infinitely thin Debye layers, through a uniform capillary with a zeta-potential that varies only in the axial direction. Ajdari (1995, 1996) and Long, Stone & Ajdari (1999) have investigated the problem of flow modification due to variable zeta-potentials for flow between parallel plates. Stroock *et al.* (2000) reported observations of electro-osmotic flow in a long channel of rectangular cross-section with a patterned surface charge of alternating sign that was fabricated using soft lithographic techniques. The problem of electro-osmotic flow in a straight micro-channel of arbitrary cross-sectional geometry and zeta-potential distribution has recently been presented by Ghosal (2002*c*), in the 'lubrication approximation' which requires that any variation of the cross-sectional shape, area or the zeta-potential in the axial direction should take place on a length scale that is very much larger than a characteristic channel radius. The dispersion of analytes caused by such variability in the wall zeta-potential has not been investigated however.

In the next section a mathematical formulation of the problem of analyte dispersion in CZE due to wall adsorption is presented. The assumption of 'slow variations' is invoked in § 3 to derive the asymptotic result mentioned earlier. In § 4 the reduced equation is solved numerically and its predictions are discussed in the light of known observations. Conclusions are summarized in § 5.

2. Mathematical formulation

Let us consider a uniform-bore capillary of radius a_0 (figure 1). We will adopt a_0 as our unit of length and a_0/u_e as our unit of time, where u_e is given by (1.1) and

ζ_* is the zeta-potential of the uncontaminated capillary. Let us adopt a cylindrical coordinate system (r, θ, x) with the origin at the inlet and x-axis along the centreline of the capillary. Then the inner surface of the capillary is at $r = 1$, the inlet is at $x = 0$ and the outlet is at $x = L$, where $L \gg 1$. We will assume that the concentration of all chemical species in solution is normalized by a single reference value c_* (the number of moles per unit volume), and the corresponding adsorbed concentrations at the walls are all normalized by $c_* a_0$ (the number of moles per unit area).

Then the concentration of any particular species, c, obeys the advection–diffusion equation

$$\frac{\partial c}{\partial t} + (\boldsymbol{u} + u_{ep}\hat{\boldsymbol{x}}) \cdot \nabla c = Pe^{-1} \nabla^2 c, \tag{2.1}$$

where $u_{ep} = v_e/u_e$ is the dimensionless electrophoretic migration velocity of the species, $Pe = a_0 u_e / D$ is its Péclet number and D is its molecular diffusion coefficient. The diffusive flux of any species is assumed to be unaffected by the presence of other species in the sample, an assumption that is valid provided the sample is sufficiently dilute. The assumption of the sample being dilute also eliminates other physical effects such as variations in the electric field strength caused by the dependence of the electrical conductivity on sample concentration. The latter effect could be important at high sample concentrations (Mikkers, Everaerts & Verheggen 1979) and is itself a source of band broadening. In (2.1) the hydrodynamic velocity is $\boldsymbol{u}$. In the absence of adsorption, $\boldsymbol{u} = \hat{\boldsymbol{x}}$; however in general $\boldsymbol{u}$ must be obtained by solving the equations for mass and momentum conservation of the fluid. The loss of analyte to the wall is described by the boundary condition:

$$-Pe^{-1} \left. \frac{\partial c}{\partial r} \right|_{r=1} = \frac{\partial s}{\partial t} \tag{2.2}$$

where s is the adsorbed concentration of the species at the wall. In order to complete the description we need a law of wall adsorption which we will write in the general form

$$\frac{\partial s}{\partial t} = f(s, c_w, \cdots). \tag{2.3}$$

Here $c_w = c(1, x, t)$ is the concentration at the wall and '$\cdots$' indicates that the rate of adsorption at the wall of a given species could depend on the concentration at the wall of all of the other species and could possibly also have an explicit dependence on position and time. The analysis presented in this paper does not require us to make any specific assumptions about the functional form of f. In practice, one often uses the 'Langmuir law' for f, which is

$$f = K_a c_w (s_m - s) - K_d s \tag{2.4}$$

where K_a and K_d are adsorption and desorption coefficients characterizing the interactions of the species with the wall material. We will also adopt this form in the numerical calculations in § 4. Since adsorption at the wall alters the wall zeta-potential, the zeta-potential is in general a function of position and time:

$$\zeta = g(s, \cdots) \tag{2.5}$$

where the function g describes the effect of the adsorbed species on the zeta-potential. Here '$\cdots$' denotes the adsorbed concentrations of all of the other species and possibly an explicit position and time dependence as well (e.g. if the capillary was already contaminated at $t = 0$). Since the zeta-potential is proportional to the

surface concentration of charge, g will usually be a linear function of the adsorbed concentration s of charged species.

In the limit of an infinitesimally thin Debye layer, the electro-osmotic effect may be incorporated in the hydrodynamic equations through the Helmholtz–Smoluchowski 'slip' boundary condition (see Probstein 1994):

$$\boldsymbol{u}|_{r=1} = \zeta \hat{\boldsymbol{x}}, \tag{2.6}$$

where ζ is the zeta-potential normalized by ζ_*. Inside the capillary, the hydrodynamic velocity, $\boldsymbol{u}$, satisfies the constant-density Navier–Stokes equations

$$Re(\partial_t \boldsymbol{u} + \boldsymbol{u} \cdot \nabla \boldsymbol{u}) = -\nabla p + \nabla^2 \boldsymbol{u}, \tag{2.7}$$

$$\nabla \cdot \boldsymbol{u} = 0, \tag{2.8}$$

where $Re = (a_0 u_e \rho_0)/\mu$ is the Reynolds number, ρ_0 is the density of the liquid and p is the pressure in units of $\mu u_e / a_0$. In microfluidic applications usually $Re \sim 10^{-3}$–1, so for generality we will assume that $Re \sim O(1)$. For an uncontaminated capillary, $\zeta = 1$, therefore (2.6)–(2.8) imply $\boldsymbol{u} = \hat{\boldsymbol{x}}$, provided there is no externally applied pressure gradient so that the pressure gradient term in (2.7) is zero.

The formulation (2.6)–(2.8) may be regarded as the lowest-order approximation to the coupled Navier–Stokes and Poisson–Boltzmann equations describing electro-osmotic effects near rigid boundaries with respect to the parameter (λ_D/a), where λ_D is the Debye length and a is the smallest geometrical length scale in the problem. Asymptotic analysis (Anderson 1985) with respect to the parameter λ_D/a shows the existence of a boundary layer of physical thickness of the order of λ_D within which electrical forces on the charged free ions are balanced by viscous forces. Outside this boundary layer the fluid may be regarded as electrically neutral, with the asymptotic matching condition (2.6). In CZE, $a \sim a_0 \sim 10$–$100\,\mu$m and $\lambda_D \sim 1$–$10\,$nm so that $\lambda_D/a \sim 10^{-3}$–10^{-5}. Thus, the assumption of an infinitely thin Debye layer is an excellent approximation.

3. The limit of slow variations

The equations presented in the last section, together with appropriate boundary and initial conditions, should provide a complete specification of the problem. However, on account of the smallness of the capillary radius in comparison to its length ($L \sim 10^3$–10^5), direct numerical integration is inefficient. This disparity in scales can be exploited however to derive a reduced description of the system that only involves solving a partial differential equation in one space variable. This is done next.

We will consider the limit when axial variations in all dependent variables occur on a characteristic length scale that is very much larger than a_0 and all temporal variations occur on a characteristic time scale that is very much larger than the diffusion time $t_D \sim a_0^2/D$, where D is the diffusivity of the slowest diffusing component in the sample. Evidently, these assumptions are not necessarily true at the time of injection, since the initial distribution of analyte concentration can be quite arbitrary, and may very well have a characteristic length scale for variation in the axial direction that is much smaller than a_0. However, as the plug is advected downstream with the characteristic speed, u_e, it undergoes diffusive spreading. As a result, Fourier-modes of wavenumber k are damped by the exponential factor $\exp[-2Dk^2 t]$. The limit of 'slow' variations as defined above is reached after a time interval such that $2Dk_m^2 t \gg 1$, where $k_m = \pi/a_0$, that is, when $t \gg t_D$. In this time, the sample has moved a distance $x \gg x_m$ from the injection point, where $x_m = a_0 Pe$. However, this requirement alone is not sufficient to

ensure slow variations since the dynamics of the adsorption process also defines a chemical time scale, t_c, that depends on the function f in equation (2.3). In particular, for the Langmuir form, (2.4), $t_c \sim K_a^{-1} t_D$. For the assumption of slow variations to be applicable, we must have $t_c/t_D \sim K_a^{-1} \gg 1$. In the language of combustion theory, K_a is a 'Damköhler number' and the above requirement is just the opposite of the limit usually studied in combustion. In CZE the characteristic adsorption times are of the order of the transit time, $t_c \sim L_0/u_e$, where L_0 is the capillary length in physical units. Indeed, if t_c is much smaller than this, then no sample will be detected at all and if it is much larger then adsorption is not of significance. Therefore $t_c \gg t_D$ requires that $(L_0/a_0)Pe^{-1} \gg 1$ or $L_0 \gg a_0 Pe$. This condition also ensures that $x_m \ll L_0$ so that the assumption of slow variations is valid everywhere except for a relatively short region near the inlet section. In CZE, $L = L_0/a_0 \sim 10^4$–10^5 whereas $Pe \sim 10$–100. Thus, the requirement $L_0 \gg a_0 Pe$ is satisfied. In equation (2.5) we have allowed ζ to depend explicitly on space and time in addition to its dependence on s. Obviously, for our analysis to be valid, any such spatial variations must be on a length scale much larger than a_0 and any such temporal variations must have a characteristic time scale much larger than t_D. Further, our analysis is not valid within a distance from the outlet that is comparable to the capillary radius as in this region the dependent variables undergo rapid variations to adjust to the conditions at the outlet reservoir.

3.1. *Asymptotic theory*

We now consider the limit of slow axial variations by postulating that our dependent variables are functions of r and the slow variables $T = \epsilon t$ and $X = \epsilon x$, where ϵ is a small parameter. The equation of continuity then requires that $\tilde{v} = v/\epsilon$ and $\tilde{p} = \epsilon p$ be of order unity, where v is the radial component of $\boldsymbol{u}$. Slow variations in s also require that f in equation (2.3) be of order ϵ. It is therefore convenient to define $\tilde{f} = f/\epsilon$, where $\tilde{f}$ is of order unity. We look for solutions satisfying this requirement of slow variations by re-writing equations (2.1)–(2.8) in terms of the variables $r, X, T, c, u, \tilde{v}, \tilde{p}$ and $\tilde{f}$, where u denotes the axial component of $\boldsymbol{u}$, and expanding all dependent variables in asymptotic series in powers of ϵ, in the form $\phi = \phi_0 + \epsilon\phi_1 + \epsilon^2\phi_2 + \cdots$ $(\phi_0 \neq 0)$.

3.1.1. *Lubrication flow*

Let us first consider the flow field. The equations for determining each succesive term in the asymptotic series may be obtained from equations (2.6), (2.7) and (2.8) by equating coefficients of successive powers of ϵ to zero. Thus, at lowest order, we obtain

$$-\frac{\partial \tilde{p}_0}{\partial X} + \frac{1}{r}\frac{\partial}{\partial r}\left(r\frac{\partial u_0}{\partial r}\right) = 0, \tag{3.1}$$

$$-\frac{\partial \tilde{p}_0}{\partial r} = 0, \tag{3.2}$$

$$\frac{\partial u_0}{\partial X} + \frac{1}{r}\frac{\partial}{\partial r}(r\tilde{v}_0) = 0, \tag{3.3}$$

$$u_0(1, X, T) = \zeta_0(X, T), \tag{3.4}$$

$$\tilde{v}_0(1, X, T) = 0. \tag{3.5}$$

These equations are simply the well-known lubrication limit of the equations of incompressible hydrodynamics. Solutions have been presented by the author in the general case of arbitrary channel geometries (Ghosal 2002*c*). For a uniform cylindrical

capillary the solution is

$$u_0 = \zeta_0 - 2(1 - r^2)(\zeta_0 - \overline{u}_0), \tag{3.6}$$

$$\tilde{v}_0 = \tfrac{1}{2} r(1 - r^2)\partial_X \zeta_0, \tag{3.7}$$

where $\overline{u}_0$ is the mean flow rate. The mean flow rate can be related to the zeta-potential,

$$\overline{u}_0 = \frac{\Delta p}{8L} + \langle \zeta_0 \rangle. \tag{3.8}$$

where $\Delta p = p(0) - p(L)$ is the applied pressure drop (if any) across the capillary. In CZE usually $\Delta p = 0$. In equations (3.6) and (3.8) and throughout this paper, the overbar will denote an average over the cross-section and the angular brackets will denote an average over the capillary length. Thus, for any variable $F(r, X, T)$,

$$\overline{F} = 2 \int_0^1 r F \, \mathrm{d}r, \tag{3.9}$$

$$\langle F \rangle = \frac{1}{L} \int_0^L F \, \mathrm{d}z. \tag{3.10}$$

In the following analysis, the correction to the lubrication-theory mass flow rate $\overline{u}_1$ will be needed. In order to calculate it, we need to solve the hydrodynamic equations at the next order. This is straightforward in principle; the calculations are presented in the Appendix. Here we simply write down the final result:

$$\overline{u}_1 = \langle \zeta_1 \rangle - \frac{1}{48} Re \frac{\mathrm{d}}{\mathrm{d}T} \left(\frac{\Delta p}{L} \right) - \frac{1}{8} Re \frac{\mathrm{d}\langle \zeta_0 \rangle}{\mathrm{d}T}. \tag{3.11}$$

For generality we have allowed the imposed pressure gradient Δp to be time dependent. Obviously any temporal variation needs to take place on a time scale that is slow in relation to the diffusion time t_D.

3.1.2. *Analyte concentration*

We now consider equations (2.1) and (2.2) rewritten in terms of the slow and fast variables

$$\frac{1}{r} \frac{\partial}{\partial r} \left(r \frac{\partial c}{\partial r} \right) = \epsilon Pe(\partial_T c + u_{ep} \partial_X c + u \partial_X c + \tilde{v} \partial_r c) - \epsilon^2 \partial_{XX} c, \tag{3.12}$$

$$-Pe^{-1} \left(\frac{\partial c}{\partial r} \right)_{r=1} = \epsilon \partial_T s. \tag{3.13}$$

At lowest order, we obtain (3.12) and (3.13) for c_0 but with a zero right-hand side. The solution, subject to the condition that there be no singularity on the axis, is $c_0 = c_0(X, T)$, that is, c_0 is independent of r. At the next order, we obtain an equation for c_1:

$$\frac{1}{r} \frac{\partial}{\partial r} \left(r \frac{\partial c_1}{\partial r} \right) = Pe[\partial_T c_0 + u_0 \partial_X c_0 + u_{ep} \partial_X c_0], \tag{3.14}$$

$$-Pe^{-1} \left(\frac{\partial c_1}{\partial r} \right)_{r=1} = \partial_T s_0. \tag{3.15}$$

If we average both sides of (3.14) over the cross-section of the capillary, the left-hand side, on using the boundary condition (3.15) and the requirement that $\partial_r c_1$ be finite on

the axis, becomes $-2\,Pe\,\partial_T s_0$. Thus, equations (3.14)–(3.15) have a solution provided the following solvability condition is satisfied:

$$\partial_T c_0 + (\overline{u}_0 + u_{ep})\partial_X c_0 = -2\partial_T s_0, \tag{3.16}$$

giving us an evolution equation for c_0.

Physically this equation indicates that the analyte band will move with a velocity $\overline{u}_0 + u_{ep}$, the algebraic sum of the bulk electro-osmotic flow speed and the electrophoretic migration speed, and, if $\partial_T s_0$ is a positive quantity (adsorption), the concentration of the analyte in the band will decay. Note that equation (3.16) does not lead to any dispersion or band broadening. In order to recover those effects, we must go to a higher order in the expansion. This we do next, but first we write down the solution to equations (3.14) and (3.15), the existence of which is now assured by the solvability condition (3.16). By straightforward integration with respect to r,

$$c_1(r, X, T) = c_1(0, X, T) - \frac{Pe}{2} r^2\,\partial_T s_0 - \frac{Pe}{8}(\zeta_0 - \overline{u}_0) r^2 (2 - r^2)\,\partial_X c_0. \tag{3.17}$$

If we average both sides of this equation over the cross-section of the capillary, the concentration on the centreline, $c_1(0, X, T)$ may be expressed in terms of $\overline{c}_1(X, T)$,

$$c_1(0, X, T) = \overline{c}_1 + \frac{Pe}{4}\partial_T s_0 + \frac{Pe}{12}(\zeta_0 - \overline{u}_0)\,\partial_X c_0, \tag{3.18}$$

so that equation (3.17) may also be written as

$$c_1(r, X, T) = \overline{c}_1(X, T) + \frac{Pe}{4}(1 - 2r^2)\,\partial_T s_0 + \frac{Pe}{24}(2 - 6r^2 + 3r^4)\,(\zeta_0 - \overline{u}_0)\partial_X c_0. \tag{3.19}$$

To obtain an evolution equation for c_1 we need to consider the order ϵ^2 terms in (3.12) and (3.13), which give

$$\frac{1}{r}\frac{\partial}{\partial r}\left(r\frac{\partial c_2}{\partial r}\right) = Pe[\partial_T c_1 + u_0\partial_X c_1 + u_{ep}\partial_X c_1 + \tilde{v}_0\partial_r c_1 + u_1\partial_X c_0 + \tilde{v}_1\partial_r c_0] - \partial_{XX} c_0, \tag{3.20}$$

$$-Pe^{-1}\left(\frac{\partial c_2}{\partial r}\right)_{r=1} = \partial_T s_1. \tag{3.21}$$

On averaging both sides of (3.20) over the cross-section and using the boundary condition (3.21) we obtain the solvability condition

$$\partial_T \overline{c}_1 + \overline{u_0\partial_X c_1} + u_{ep}\partial_X \overline{c}_1 + \overline{\tilde{v}_0\partial_r c_1} + \overline{u}_1\partial_X \overline{c}_0 + 2\partial_T s_1 - Pe^{-1}\partial_{XX}\overline{c}_0 = 0, \tag{3.22}$$

where we have made use of the fact that c_0 is a function of X and T only, so that $\partial_r c_0 = 0$ and $c_0 = \overline{c}_0$. On substituting the expressions for u_0, $\tilde{v}_0$, and c_1 from equations (3.6), (3.7) and (3.19) into (3.22) and evaluating the cross-sectional averages, we arrive at the following equation for $\overline{c}_1$;

$$\partial_T \overline{c}_1 + (u_{ep} + \overline{u}_0)\partial_X \overline{c}_1 + 2\partial_T s_1 = -\overline{u}_1\partial_X \overline{c}_0 + Pe^{-1}\partial_{XX}\overline{c}_0 + \frac{Pe}{12}\partial_X[(\zeta_0 - \overline{u}_0)\partial_T s_0] + \frac{Pe}{48}\partial_X[(\zeta_0 - \overline{u}_0)^2\partial_X \overline{c}_0]. \tag{3.23}$$

3.2. *Evolution equations for $\overline{c}$ and s*

It is possible to combine the evolution equations for $\overline{c}$ at zeroth and first order to obtain a single equation for $\overline{c}$. This is achieved by multiplying (3.23) by ϵ and adding the result to (3.16) and remembering that higher-order terms may be added

or dropped without affecting the asymptotic validity of the resulting equation. Thus, we obtain

$$\frac{\partial \overline{c}}{\partial t} + (\overline{u} + u_{ep})\frac{\partial \overline{c}}{\partial x} = \frac{\partial}{\partial x}\left(\mathscr{D}\frac{\partial \overline{c}}{\partial x}\right) + \mathscr{G} \tag{3.24}$$

where

$$\overline{u} = \frac{\Delta p}{8L} + \langle \zeta \rangle - \frac{1}{8}Re\frac{\mathrm{d}\langle \zeta \rangle}{\mathrm{d}t} - \frac{1}{48}Re\frac{\mathrm{d}}{\mathrm{d}t}\left(\frac{\Delta p}{L}\right) \tag{3.25}$$

is the bulk flow speed,

$$\mathscr{D} = \frac{1}{Pe} + \frac{Pe}{48}(\zeta - \overline{u})^2 \tag{3.26}$$

is an 'effective' diffusivity and

$$\mathscr{G} = -2\frac{\partial s}{\partial t} + \frac{Pe}{12}\frac{\partial}{\partial x}\left[(\zeta - \overline{u})\frac{\partial s}{\partial t}\right] \tag{3.27}$$

is a source term that is reponsible for the removal of analyte from the buffer. We have now reverted to our original independent variables r, x and t so that ϵ no longer appears explicitly in these equations. The zeta-potential is given by (2.5) as a function of the adsorbed species concentrations, $\zeta = g(s, \cdots)$.

The distribution of concentration may be found from $c = c_0 + \epsilon c_1 + \cdots$, and equation (3.19):

$$c = \overline{c}(x, t) + \frac{Pe}{4}(1 - 2r^2)\,\partial_t s + \frac{Pe}{24}(2 - 6r^2 + 3r^4)\,(\zeta - \overline{u})\partial_x \overline{c}. \tag{3.28}$$

This expression is asymptotically correct to order ϵ. The value of c at the wall is obtained by setting $r = 1$, thus

$$c_w = \overline{c}(x, t) - \frac{Pe}{4}\,\partial_t s - \frac{Pe}{24}\,(\zeta - \overline{u})\partial_x \overline{c}. \tag{3.29}$$

In order to determine an equation for s, we substitute equation (3.29) in (2.3), and Taylor expand f with respect to the variables c_w corresponding to each species, keeping only the leading-order term:

$$\frac{\partial s}{\partial t} = f(s, \overline{c}, \cdots) + \sum_{*}\left\{-\frac{Pe^*}{4}\,\partial_t s^* - \frac{Pe^*}{24}\,(\zeta - \overline{u})\partial_x \overline{c}^*\right\} \quad \partial_{c_w^*} f\big|_{c_w^* = \overline{c}^*}. \tag{3.30}$$

Here the summation indicated runs over all species indexed by the superscript $*$. Since $\partial_t s^* = f^*(s, \overline{c}, \cdots)+$ higher-order terms, we may rewrite (3.30) as follows:

$$\frac{\partial s}{\partial t} = f(s, \overline{c}, \cdots) - \sum_{*}\frac{Pe^*}{4}\; f^*\partial_{c_w^*} f\big|_{c_w^* = \overline{c}^*} - \sum_{*}\frac{Pe^*}{24}(\zeta - \overline{u})\partial_x \overline{c}^*\;\partial_{c_w^*} f\big|_{c_w^* = \overline{c}^*} \tag{3.31}$$

Equation (3.28) determines the three-dimensional distribution of concentration in terms of the variables $\overline{c}$ and s which evolve in time according to equations (3.24) and (3.31). These equations have an asymptotic validity to terms of $O(\epsilon^2)$. This is the main results of this paper. Equation (3.24) shows that $\overline{c}$ obeys an advection–diffusion equation with a source/sink term to account for wall adsorption effects. The mean concentration is advected by the bulk flow speed $\overline{u}$, as in classical Taylor dispersion theory, corrected by the electrophoretic migration velocity u_{ep}. The effective axial diffusion coefficient $\mathscr{D}$ in equation (3.26) is simply the sum of the molecular diffusivity and the classical expression for the Taylor diffusion coefficient evaluated using only

Case	K_a	K_d	$s_m \times 10^3$
O	0	0	10.0
I	0.02	0	10.0
II	0.10	0	1.0
III	0.125	0.0001	0.8

TABLE 1. Parameters values for numerical simulations.

the Poiseuille part of the expression for the axial velocity in equation (3.6). This is what one might expect intuitively in the limit of slow axial variations. The source term on the right of (3.24) represents losses to the wall. If the sample is far enough from the inlet or outlet so that sample concentrations are essentially zero at $x = 0$ and $x = L$, then we may integrate (3.24) to arrive at the conservation law

$$\frac{\mathrm{d}}{\mathrm{d}t}\left[\int_0^L (c + 2s)\,\mathrm{d}x\right] = 0, \tag{3.32}$$

which simply indicates that any decrease of a sample component in solution is accounted for by the corresponding amount adsorbed at the wall. The second term, proportional to the Péclet number in equation (3.27) is a correction to the wall flux because the sample concentration is not exactly uniform over the capillary cross-section. Similarly, the terms proportional to the Péclet number in equation (3.31) account for the fact that the concentration of each of the species at the wall differs slightly from the mean concentration at each cross-section.

4. Numerical solutions

We will now investigate the consequences of the equations presented in § 3.2, by numerically integrating these equations under conditions fairly representative of CZE in the presence of wall adsorption. It will be seen that these equations provide a rational basis for understanding many of the qualitative features observed in practice.

The numerical integration was carried out† with a finite-difference method that uses sixth-order central differencing to compute the spatial derivatives and uses explicit time marching with the fourth-order Runge–Kutta method. The sample calculations are for a single species. Zero boundary conditions for the concentrations $\bar{c}$ and s are assumed at the lateral boundaries, $x = 0$ and $x = L$. For initial conditions a Gaussian profile is used for $\bar{c}$, $\bar{c}(x, 0) = c_m(0) \exp\left[-(x - x_0)^2/(2\sigma_0^2)\right]$, with $c_m(0) = 1$, $\sigma_0 = 10$, $x_0 = 5\sigma_0$ and we assume $s(x, 0) = 0$. The capillary length is $L = 10^4$ and the calculation is stopped when the concentration peak reaches a detector that we will assume is located at $x = x_d = 9000 = L - 100\sigma_0$. The values of x_0 and x_d have been chosen so that the analyte is always localized sufficiently far from the inlet and outlet boundaries. This ensures that the computation is insensitive to the choice of inlet and outlet boundary conditions for $\bar{c}$. The Langmuir form (2.4) is assumed for the wall interaction. Four cases are run with values of the parameters K_a, K_d and s_m as shown in table 1. These parameters are chosen keeping in mind that consistent with the requirement of slow variations, $K_a^{-1} \sim K_d^{-1} \gg 1$, but still small enough to have

† A computer program for one-dimensional flame calculations kindly provided by Professor Luc Vervisch was modified for the purpose.

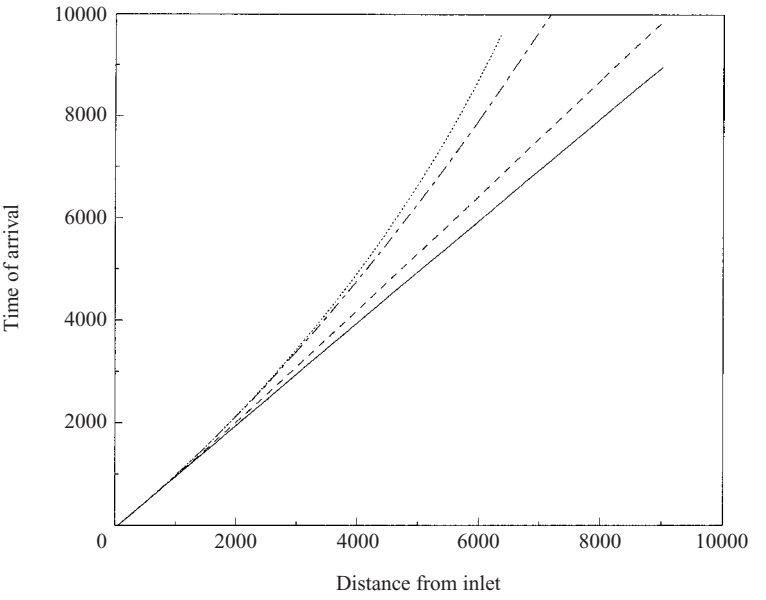

FIGURE 2. Arrival times of the analyte peak as a function of distance from inlet of the capillary for numerical simulations using parameter values shown in table 1 (Case O: ———, Case I: – – – –, Case II: ·····, Case III: — – —).

observable effects. Further, since the total adsorbed analyte must be of the order of the amount injected, $2\pi s_m L \sim c_m(0)\sigma_0$. The dependence of ζ on s is taken as

$$\zeta = g(s, \cdots) = 1 - s/s_m \tag{4.1}$$

so that (i) $\zeta = 1$ if $s = 0$, (ii) ζ decreases linearly with s, and (iii) adsorption stops when $\zeta = 0$ (at $s = s_m$) which corresponds to neutralization of the charge on the capillary wall. The Reynolds number, Re is taken to be zero in these examples and the Péclet number $Pe = 100$. These conditions are fairly typical in CZE (Landers 1996; Camilleri 1998). Since the electrophoretic migration velocity u_{ep} simply results in a constant increment to the propagation velocity of the band, we take $u_{ep} = 0$ in these calculations for the sake of convenience.

Adsorption of analytes to channel walls is known to result in altered elution times for analyte bands (Towns & Regnier 1992). Figure 2 shows this effect. The time of arrival of the analyte concentration peak at a given location x is shown. In the absence of adsorption (Case O), the band simply moves with a uniform velocity of unity. In all other cases, the elution times are increased. This is a consequence of the reduction in the ζ-potential behind the band, as a result of which the bulk flow velocity, which is proportional to the axial average of the zeta-potential, decreases with time as well. In Ghosal (2002*b*), an *ad hoc* exponential model was proposed for the zeta-potential in the wake of the analyte band while ahead of it the value for an uncontaminated capillary was assumed. This, together with (3.25), was used to derive an analytical formula for elution times which could be fitted well to experimental data. Here we have obtained similar qualitative results but without any *ad hoc* assumptions about how the zeta-potential is altered. The actual form of the zeta-potential at the instant the analyte peak reaches the detector is shown in figure 5 for each of the calculations in table 1. It is clear that the exponential model used in Ghosal (2002*b*) provides

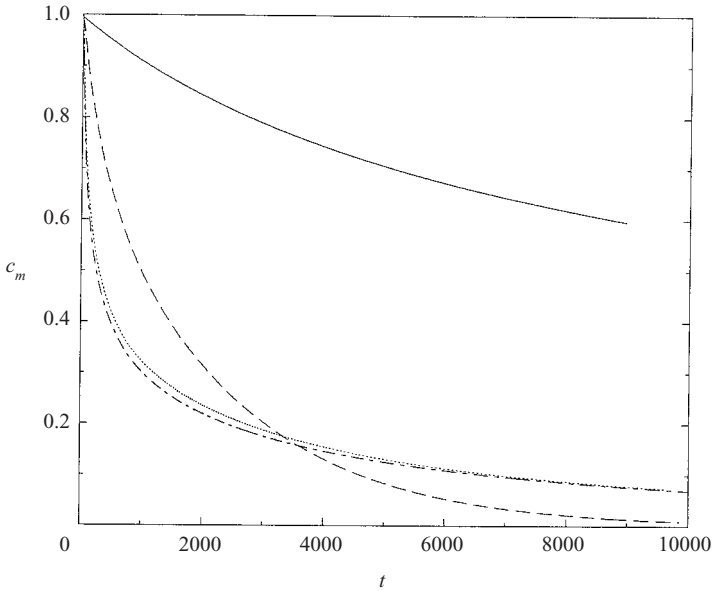

FIGURE 3. Peak sample concentration $c_m(t)$ as a function of time t for numerical simulations using parameter values shown in table 1 (Case O: ———, Case I: – – – –, Case II: ·····, Case III: — – —). The peak concentration shows a rapid decrease with time when wall adsorption is present, due to the combined effect of analyte loss and enhanced dispersion.

a fair description of $\zeta(x)$ only for Case I where the adsorbed concentration is low enough that saturation levels are not reached.

Figure 3 shows the decrease in the peak value of the concentration c_m with time, t. In Case O the decrease is solely due to the spreading of the band on account of molecular diffusion and the constraint of mass conservation. In the remaining three cases, the peak concentration decays due to a combination of dispersion and loss of analyte to the wall. Clearly, wall interactions lead to a very large decrease in c_m. In many instances this decrease is so large that the concentration falls below the threshold of detection at the detector window.

In figure 4, the concentration profile at the instant the peak reaches the detector is shown for all four Cases displayed in table 1. For ease of comparison, the profiles are normalized so that the maximum value is unity in all of the cases. Clearly, the narrowest peak is obtained in Case O. In all of the other cases, analyte adsorption broadens the peak to various degrees. It is interesting to note that in the presence of adsorption, the peaks take on a markedly asymmetric shape. This is in accordance with observations in CZE where such 'eluted peaks' are considered an indicator of the presence of strong wall interactions. It is significant that the asymmetry is present even if $K_d = 0$. Thus, the analyte desorbing behind the moving plug appears not to be the primary cause of peak asymmetry. In addition to the 'eluted peaks' Case III shows that the concentration does not quite return to zero after passage of the peak, but shows a plateau that continues for many profile widths behind the peak. This is also in accord with a well-known effect in CZE, where it has been noted that in the presence of significant wall interactions, there is a 'lack of return to the baseline' of the detector signal.

Finally, figure 5 shows the zeta-potential in all four cases at the instant the analyte peak reaches the detector. The curve $\zeta = 1$ corresponds to Case O (no adsorption).

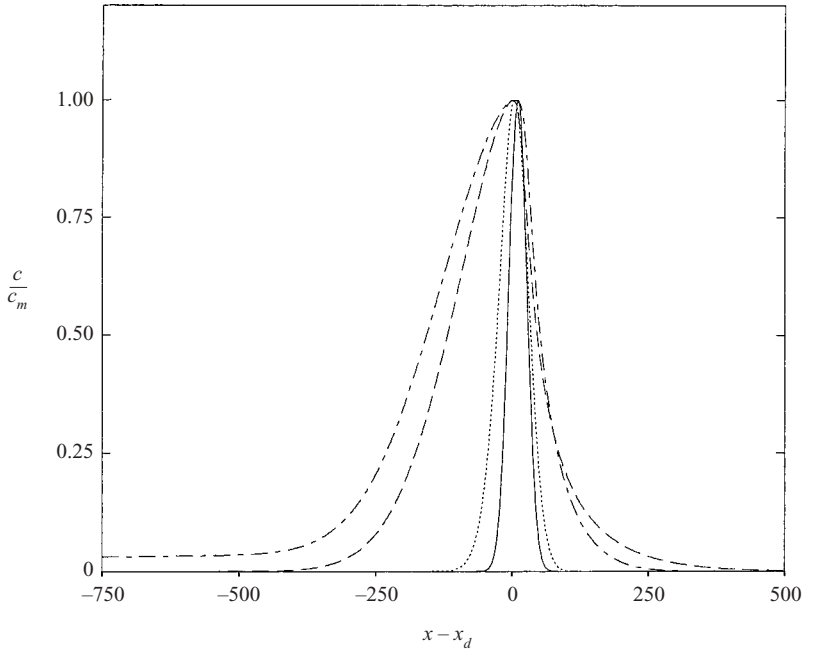

FIGURE 4. Axial profiles of the normalized mean concentration ($\overline{c}/c_m$), for numerical simulations using parameter values shown in table 1 (Case O: ———, Case I: ·····, Case II: – – – –, Case III: — – —) at the instant the analyte peak reaches the detector. Note that in the presence of wall interactions (Case I, II and III) peak shapes are asymmetric. In the presence of desorption (Case III) the peak has a long plateau behind it, so that the signal does not return to the 'base-line' for a long time after passage of the analyte peak.

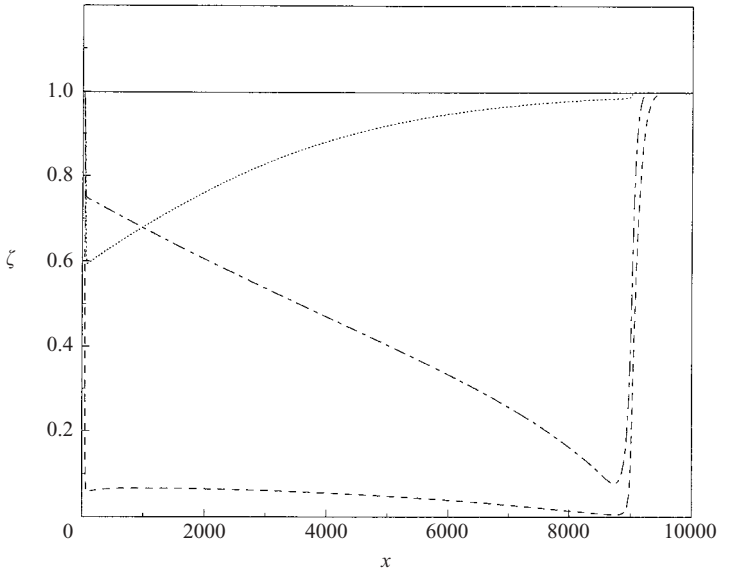

FIGURE 5. Profiles of the zeta-potential (ζ), for numerical simulations using parameter values shown in table 1 (Case O: ———, Case I: ·····, Case II: – – – –, Case III: — – —) at the instant the analyte peak reaches the detector.

From (4.1), $s = s_m(1 - \zeta)$ so that the area enclosed by the curves $\zeta(x)$ and $\zeta = 1$ between x and $x + \mathrm{d}x$ is proportional to the analyte adsorbed in the section of length $\mathrm{d}x$ on the capillary. In Case I the amount adsorbed per unit length decreases with distance from the inlet. This is because the rate of adsorption is proportional to the concentration in the band and this concentration decreases with time as the sample moves towards the outlet. In Case II $\zeta \approx 0$ behind the sample due to strong adsorption. In this case, the adsorbed concentration per unit length actually increases slightly with distance from the inlet. This is a result of the slowing down of the plug (see figure 2) due to the reduction of $\overline{u} = \langle \zeta \rangle$ with time. As a result the plug takes a much longer time to pass a fixed point on the wall so that the time available for adsorption is much greater for downstream points. This effect more than compensates for the depletion of analyte concentration in the plug. In Case III, each point on the wall adsorbs analyte as the plug passes over it but subsequently the analyte is slowly released back into the buffer due to desorption. This accounts for the 'recovery' of the zeta-potential in the wake of the plug. It also accounts for the very long plateau behind the concentration peak in figure 4 for Case III. As a result of this recovery, $\langle \zeta \rangle$ is much larger in Case III than in Case II so that elution time delays (figure 2) are less pronounced.

5. Conclusion

The problem of the anomalous dispersion of analytes in CZE due to wall interactions was investigated using a rational approximation. The analysis invoked the following assumptions:

(*a*) The Debye layer thickness is very much smaller than the capillary radius, so that the Helmholtz–Smoluchowski slip boundary conditions are adequate for describing the coupling between the electric field and the fluid flow.

(*b*) The capillary length $L_0 \gg a_0 Pe$, where a_0 is the capillary radius and Pe is the Péclet number of the slowest diffusing species that has significant wall interactions.

(*c*) The characteristic chemical time scale defining the adsorption rate is comparable to the transit time across the capillary.

(*d*) Any explicit axial variations in the zeta-potential, if present, have a characteristic length scale much larger than a_0. Any explicit temporal variations in the zeta-potential or applied pressure head, if present, are slow compared to the diffusive time across a capillary radius.

The principal results of the paper are equations (3.28), (3.24) and (3.31). These coupled partial differential equations for $\overline{c}$ and s must in general be solved numerically. However, since they involve only one space variable they represent a considerable simplification over the full three-dimensional formulation.

This reduced system of equations was solved numerically using parameter values that would be typical for CZE. It was found that the solution displayed most of the characteristics exhibited by CZE systems in the presence of wall interactions that are known from empirical observations. In particular, the presence of wall interactions results in increased elution times, peak broadening, an asymmetrical peak shape often referred to as 'peak tailing' and 'lack of return to the baseline' of the signal after passage of the primary pulse. It would be of interest to make a quantitative comparison of these predictions with experimental data. This has been attempted in some cases (Ghosal 2002*a*, *b*) using semi-empirical models, for which the present paper provides a rational basis.

A part of this research was conducted at the NASA Ames Research Center, Mountainview, CA where the author was supported during the summer of 2002 through the NASA-ASEE-SJSU Faculty Fellowship Program (NFFP). The author is also pleased to acknowledge numerous fruitful discussions with his NASA host Dr Karim Shariff.

Appendix. Correction to the lubrication approximation

The lubrication approximation is the lowest-order approximation to (2.6)–(2.8). At the next order, (2.7) and (2.8) give

$$\frac{1}{r}\frac{\partial}{\partial r}\left(r\frac{\partial u_1}{\partial r}\right) - \frac{\partial \tilde{p}_1}{\partial X} = Re\left[\frac{\partial u_0}{\partial T} + u_0\frac{\partial u_0}{\partial X} + \tilde{v}_0\frac{\partial u_0}{\partial r}\right], \tag{A 1}$$

$$\frac{\partial \tilde{p}_1}{\partial r} = 0. \tag{A 2}$$

Equation (A 2) implies that $p_1 = p_1(X, T)$; further the right-hand side of (A 1) may be evaluated using the lower-order solution (3.6) and (3.7):

$$\frac{1}{r}\frac{\partial}{\partial r}\left(r\frac{\partial u_1}{\partial r}\right) = \partial_X \tilde{p}_1 + Re[2r^4(\zeta_0 - \overline{u}_0)\partial_X\zeta_0 + 2(1-r^2)\partial_T\overline{u}_0 + (2r^2-1)(\partial_T\zeta_0 + 2\overline{u}_0\partial_X\zeta_0 - \zeta_0\partial_X\zeta_0)]. \tag{A 3}$$

From the boundary condition (2.6),

$$u_1|_{r=1} = \zeta_1(X, T). \tag{A 4}$$

If we integrate (A 3) using boundary condition (A 4) and the requirement that there must not be a singularity at $r = 0$, we obtain

$$u_1 = \zeta_1 + \tfrac{1}{4}(r^2-1)\partial_X\tilde{p}_1 + Re\big[\tfrac{1}{18}(r^6-1)(\zeta_0 - \overline{u}_0)\partial_X\zeta_0 - \tfrac{1}{8}(r^4 - 4r^2 + 3)\partial_T\overline{u}_0 + \tfrac{1}{8}(r^2-1)^2(\partial_T\zeta_0 + 2\overline{u}_0\partial_X\zeta_0 - \zeta_0\partial_X\zeta_0)\big]. \tag{A 5}$$

To obtain the flux, we integrate over the cross-section,

$$\overline{u}_1 = \int_0^1 2ru_1\,dr = \zeta_1 - \tfrac{1}{8}\partial_X\tilde{p}_1 - Re\big[\tfrac{1}{24}(\zeta_0 - \overline{u}_0)\partial_X\zeta_0 + \tfrac{1}{6}\partial_T\overline{u}_0 - \tfrac{1}{24}(\partial_T\zeta_0 + 2\overline{u}_0\partial_X\zeta_0 - \zeta_0\partial_X\zeta_0)\big]. \tag{A 6}$$

Equation (A 6) can be solved for $\partial_X\tilde{p}_1$;

$$\frac{\partial \tilde{p}_1}{\partial X} = 8(\zeta_1 - \overline{u}_1) - Re\big[\tfrac{1}{3}(\zeta_0 - \overline{u}_0)\partial_X\zeta_0 + \tfrac{4}{3}\partial_T\overline{u}_0 - \tfrac{1}{3}(\partial_T\zeta_0 + 2\overline{u}_0\partial_X\zeta_0 - \zeta_0\partial_X\zeta_0)\big]. \tag{A 7}$$

If we average both sides over the length of the capillary and keep in mind that the pressure at each end is specified, so that $\tilde{p}_1$ is zero at the inlet and outlet, we obtain

$$\overline{u}_1 = \langle\zeta_1\rangle - \tfrac{1}{6}Re\frac{\mathrm{d}\overline{u}_0}{\mathrm{d}T} + \tfrac{1}{24}Re\frac{\mathrm{d}\langle\zeta_0\rangle}{\mathrm{d}T}. \tag{A 8}$$

In arriving at equation (A 8) we have set the integrals of the total derivative terms to zero. This is justified if $\epsilon L \gg 1$, that is, the capillary is very much longer than the

characteristic width of the analyte band. On using equation (3.8) in (A 8) we obtain

$$\overline{u}_1 = \langle \zeta_1 \rangle - \frac{1}{48} Re \frac{\mathrm{d}}{\mathrm{d}T} \left(\frac{\Delta p}{L} \right) - \frac{1}{8} Re \frac{\mathrm{d}\langle \zeta_0 \rangle}{\mathrm{d}T}. \tag{A 9}$$

This is equation (3.11) in § 3.1.1.

REFERENCES

Ajdari, A. 1995 Electro-osmosis on inhomogeneously charged surfaces. *Phys. Rev. Lett.* **75**, 755–758.

Ajdari, A. 1996 Generation of transverse fluid currents and forces by an electric field: Electro-osmosis on charge-modulated and undulated surfaces. *Phys. Rev.* E **53**, 4996–5005.

Anderson, J. 1985 Effect of nonuniform zeta potential on particle movement in electric fields. *J. Colloid Interface Sci.* **105**, 45–54.

Anderson, J. & Idol, W. 1985 Electroosmosis through pores with nonuniformly charged walls. *Chem. Engng Commun.* **38**, 93–106.

Camilleri, P. (Ed.) 1998 *Capillary Electrophoresis, Theory and Practice*. CRC Press.

Ermakov, S., Zhukov, M., Capelli, L. & Righetti, P. 1995 Wall adsorption in capillary electrophoresis experimental study & computer simulation. *J. Chromatogr.* A **699**, 297–313.

Gaš, B. & Kendler, E. 2000 Dispersive phenomena in electromigration separation methods. *Electrophoresis* **21**, 3888–3897.

Gaš, B., Štědrý, M., Rizzi, A. & Kendler, E. 1995 Dynamics of peak dispersion in capillary zone electrophoresis including wall adsorption: I. theoretical model and results of simulation. *Electrophoresis* **6**, 958–967.

Ghosal, S. 2002*a* Band broadening in a micro-capillary with a step-wise change in the ζ-potential. *Anal. Chem.* **74**, 4198–4203.

Ghosal, S. 2002*b* Effect of analyte adsorption on the electroosmotic flow in microfluidic channels. *Anal. Chem.* **74**, 771–775.

Ghosal, S. 2002*c* Lubrication theory for electroosmotic flow in a microfluidic channel of slowly varying cross-section and wall charge. *J. Fluid Mech.* **459**, 103–128.

Herr, A., Molho, J., Santiago, J., Mungal, M., Kenny, T. & Garguilo, M. 2000 Electroosmotic capillary flow with nonuniform zeta potential. *Anal. Chem.* **72**, 1053–1057.

Jakeway, S., de Mello, A. & Russell, E. 2000 Miniaturized total analysis systems for biological analysis. *Fresen. J. Anal. Chem.* **366**, 525–539.

Jorgenson, J. 1987 *New Directions in Electrophoretic Methods*, chaps. 1 and 13. American Chemical Society.

Landers, J. (Ed.) 1996 *Introduction to Capillary Electrophoresis*. CRC Press.

Long, D., Stone, H. & Ajdari, A. 1999 Electroosmotic flows created by surface defects in capillary electrophoresis. *J. Colloid Interface Sci.* **212**, 338–349.

Mikkers, F., Everaerts, F. & Verheggen, T. P. 1979 Concentration distributions in free zone electrophoresis. *J. Chromatography* **169**, 1–10.

Probstein, R. 1994 *Physicochemical Hydrodynamics*. John Wiley and Sons.

Schure, M. & Lenhoff, A. 1993 Consequences of wall adsorption in capillary electrophoresis: Theory & simulation. *Anal. Chem.* **65**, 3024–3037.

Stroock, A., Weck, M., Chiu, D., Huck, W., Kenis, P., Ismagilov, R. & Whitesides, G. 2000 Patterning electro-osmotic flow with patterned surface charge. *Phys. Rev. Lett.* **8415**, 3314–3317.

Towns, J. & Regnier, F. 1992 Impact of polycation adsorption on efficiency and electroosmotically driven transport in capillary electrophoresis. *Anal. Chem.* **64**, 2473–2478.

Štědrý, M., Gaš, B. & Kendler, E. 1995 Dynamics of peak dispersion in capillary zone electrophoresis including wall adsorption: ii. exact analysis of unsteady linear adsorptive dispersion. *Electrophoresis* **16**, 2027–2033.

Weinberger, R. 2000 *Practical Capillary Electrophoresis*. Academic.

Zhukov, M., Ermakov, S. & Righetti, P. 1997 Simplified mathematical model of irreversible sample adsorption in capillary zone electrophoresis. *J. Chromatogr.* A **766**, 171–185.